Transgenic mice overexpressing glia maturation factor-β, an oxidative stress inducible gene, show premature aging due to Zmpste24 down-regulation

Graduate School of Life Science, Kobe Women's University

Rika Imai

2015

Contents

Summary

This thesis begins with a brief introduction to glia maturation factor-β (GMF), a brain-specific protein, followed by a discussion of the physiological functions of GMF. Next, the relation between GMF and chronic kidney disease (CKD) is introduced, which will be referenced throughout this work. Briefly, GMF is ectopically induced in renal tubules by CKD associated with proteinuria. GMF overexpression in non-brain cells causes apoptosis *in vitro* via cellular vulnerability to oxidative stress. After that, the pathological roles of GMF in the neurodegenerative diseases are introduced. In the present study, we constructed transgenic mice overexpressing GMF (GMF-TG) and investigated the roles of GMF in non-brain tissues *in vivo*.

Results of the research conducted during this study are presented in Chapter 2. We evaluated the GMF-TG mice for 155 weeks and compared with the wild-type mice. The GMF-TG mice prematurely exhibited aging-associated symptoms including a lack of hair glossiness, hair graying, alopecia, skin atrophy, and curvature of the spine as seen in normal human aging. The GMF-TG mice also demonstrated short lifespans and reduced hair regrowth, suggesting an accelerated aging process.

The analysis of premature aging syndromes develops understanding of the molecular basis of the physiological aging. The production of an abnormal lamin A, a nuclear envelope protein, has been identified as the cause of accelerated aging diseases, known as laminopathies, and might play a causal role in normal aging. Some phenotypes seen in the GMF-TG mice, such as alopecia and skin atrophy were similar to those of

laminopathy-based premature aging. Here, we examined whether this accelerated aging characteristics observed in the GMF-TG mice would be associated with laminopathies. We identified the abnormal lamin A (prelamin A), accompanied by a down-regulation of a lamin A processing enzyme (Zmpste24) in the kidney of the GMF-TG mice. The GMF-TG mice showed accelerated aging in the kidney, compared with the wild-type mice, showing the increased the transforming growth factor-β1 (*TGF-β1*) and connective tissue growing factor (*CTGF*) gene expression and the decline of renal function (e.g. increased serum creatinine). The mRNA expression of p21/waf1 was increased at an earlier stage of life, at 10 weeks, which was in turn down-regulated at a later stage, at 60 weeks. In this chapter, we demonstrated the GMF-TG mice showed very mild accelerated aging phenotypes due to the abnormal lamin A, accompanied by Zmpste24 down-regulation.

In chapter 3, we proposed a novel role of GMF overexpression in non-brain tissues *in vivo*. This proposition suggests that the gene expression of Zmpste24 in the GMF-TG mice might respond sensitively to oxidative stress, which may be associated with a vulnerability to oxidative stress caused by GMF overexpression. The usefulness of the GMF-TG mice will be presented.

Chapter 1.

Introduction

1.1 Glia maturation factor-β

Glia maturation factor-β (GMF) was first detected in 1972 by Lim et al. as a consequence of search for growth or differentiation factors in the nervous system [1-3]. GMF is a 17-kDa highly conserved 141-amino acid protein, with 99% homology between humans and rodents [4]. It is localized in the cytoplasm of glial cells, mainly astrocytes, and some neurons [4-6]. GMF has no leader sequence and is not secreted by the cells [5]. GMF mRNA is predominantly expressed in the brain and spinal cord, although trace levels are found in other organs, including testis and ovary (Figure 1) [6].

It has been reported by Lim et al. that recombinant GMF can be phosphorylated *in vitro* at the serine residue by protein kinase C, protein kinase A, and casein kinase II, and at the threonine residue by p90 ribosomal S6 kinase, indicating that GMF possesses several consensus phosphorylation sites [5,7]. Protein kinase A-phosphorylated GMF inhibits the activity of mitogen-activated protein kinases (MAPK), ERK1 and ERK2 (extracellular signal-regulated kinase 1 and 2, respectively) [8], while it promotes the activity of p38-MAPK [9]. MAPK is an important signaling pathway regulating a variety of physiological processes such as cell growth, proliferation, differentiation, migration, and apoptosis [10]. The three major MAPK cascades; ERK cascade, c-Jun amino-terminal protein kinase/stress-activated protein kinase (JNK/SAPK) cascade and

p38-MAPK cascade are well-known [10]. Lim et al. [5] and Zaheer et al. [11] have demonstrated that overexpression of GMF in brain cells stimulates p38-MAPK activity and activates the transcription factor nuclear factor-κB (NF-κB). Activation of NF-κB plays a central role in the regulation of diverse cellular processes such as inflammation, immune response, differentiation, proliferation and apoptosis [12]. GMF has been currently described as an intracellular regulator of cell signal transduction.

GMF has also been identified as a member of the actin-depolymerizing factor homology (ADF-H) family [13] which regulates actin filament dynamics at multiple cellular locations [14]. Actin filament dynamics play important roles in fundamental cellular processes, including cell motility, cell division, control of cell shape and endocytosis [13,15].

1.2 Glia maturation factor-β and Chronic kidney disease

Previously Takenaka et al. [16] and Nakajima et al. [17] have shown that proteinuria induces the ectopic expression of GMF, a brain specific protein, in renal proximal tubular cells. Kaimori et al. [18] showed that GMF overexpression in non-brain cells led to vulnerability to oxidative injury through p38-MAPK pathway and changes in antioxidant enzyme activities *in vitro* (Figure 2). This function was confirmed by evidence showing that GMF-null astrocytes increased resistance to oxidative stress [19].

Oxidative stress is broadly defined as an imbalance between reactive oxygen species (ROS) production and the cellular antioxidant defense system (Figure 3) [20,21]. ROS are produced in all mammalian cells, as a consequence of normal cellular metabolism [20,22]. It is thought that oxidative stress causes damage to biomolecules such as

proteins, lipids and DNA, resulting in cellular damage and aging (Figure 3) [21,23,24].

Chronic kidney disease (CKD) is defined as abnormalities of kidney structure and/or function, present for a period of three months or more (Table I) [25]. Chronic proteinuria is not only a sign of CKD, it also plays an important role in the progression of CKD [26]. It is known that oxidative stress is elevated in patients with CKD [27,28]. Taken together, it suggests that the induction of GMF in renal proximal tubular cells by proteinuria might play a key role in the pathogenesis of CKD by enhancing oxidative injuries [18]. It is likely that GMF has the pathological functions as well as the physiological functions.

1.3 Glia maturation factor-β and Neurodegenerative disease

Recent studies had shown that GMF was up-regulated in the specific areas of Alzheimer's disease brain [29-31]. It is considered that inflammatory response of glial cells is closely intertwined with pathogenesis of neurodegenerative diseases, such as Alzheimer's disease, Parkinson's disease and Multiple sclerosis [32-36]. It has been reported that GMF induces granulocyte-macrophage colony-stimulating factor (GM-CSF) and interleukin-33 (IL-33) in astrocytes [4,34,35,37]. GMF also was associated with the proinflammatory cytokine/chemokine production, including tumor necrosis factor-α (TNF-α), interleukin-1β (IL-1β), interleukin-6 (IL-6), and interferon gamma-induced protein 10 (IP-10) in microglia [4,32-38]. It suggests that GMF overexpression in brain tissue acts as a prominent mediator of inflammatory signal transduction in the central nervous system, leading to the death of neurons in the neurodegenerative diseases (Figure 4) [4,32-38].

1.4 Focus of this thesis

Several previous studies have shown the physiological [1-8,11] and pathophysiological [4,29-38] roles of the expression of GMF in the brain tissue. However, as far as we know, the roles of GMF in the non-brain tissues have not been fully clarified. Thus the aim of the present study was to investigate the roles of GMF overexpression in non-brain tissues.

Chapter 2.

Transgenic mice overexpressing GMF, an oxidative stress inducible gene, show premature aging due to Zmpste24 down-regulation

The thesis is prepared based on the quotations from our article published in Aging.

This has been already approved by the publisher.

2.1 Introduction

The nuclear lamina is a filamentous protein meshwork underlying the inner nuclear membrane [39,40]. It plays important roles in maintaining the nuclear envelope and providing anchorage sites for chromatin [40,41]. It has been recognized that the nuclear lamina is also involved in various functions at the cellular level, including DNA replication, transcription, and apoptosis [41-43]. The major components of the nuclear lamina are intermediate filament proteins, the A- and B-type lamins [40,42]. The A-type lamins, such as lamin A and C, arise from the single gene (*LMNA* gene) by alternative splicing of the transcript [40,41]. Lamin A is derived from its precursor prelamin A, through a multi-step maturation process [39]. Zinc-metalloprotease, Zmpste24 is an enzyme required for the correct processing and maturation of lamin A [39]. The B-type lamins, such as lamin B1 and B2, are encoded by separate genes (*LMNB1* and *LMNB2*) [41].

Mutations in the gene coding the nuclear lamina components cause a wide variety of diseases known as laminopathies [42]. For example, Hutchinson-Gilford progeria syndrome (HGPS) [44] and restrictive dermopathy [45] are rare genetic accelerated aging diseases caused by mutations of the *LMNA* or *ZMPSTE24* gene. These mutations produce mutant lamin A proteins, such as progerin or prelamin A, respectively [42], which can cause disassembly of the nuclear envelope proteins, subsequently accompanied by accelerated aging due to laminopathies [42]. Laminopathies caused by the alteration of the lamin A protein and their assembly can be further classified into the primary and secondary laminopathies [42]. The primary laminopathies are due to mutations in the *LMNA* gene and the secondary laminopathies are caused by mutations

in the *ZMPSTE24* gene [42]. Laminopathies exhibit clinical features mimicking physiological aging, including sclerotic skin, joint contractures, bone abnormalities, and alopecia, but the clinical features of laminopathies are radical [42,44,45]. Interestingly, the abnormalities associated with lamin A are normally observed in healthy human aging, suggesting that the accumulation of abnormal lamin A protein is associated with organismal physiological aging [46-49].

In the present study, the first step was to construct transgenic mice overexpressing GMF (GMF-TG) in order to examine the roles of GMF in non-brain tissues *in vivo*. During the breeding period, we found that the GMF-TG mice prematurely exhibited phenotypes resembling human aging, such as alopecia and skin atrophy. These phenotypes appeared to be similar to those of laminopathy-based premature aging. We investigated the development of accelerated aging phenotypes in the GMF-TG mice.

2.2 Materials and Methods

Ethics statement

All of the animal experiments employed in this study were conducted in accordance with protocols approved by the Ethical Committee of Kobe Women's University on Animal Research (Permit Number: 154, 181, 209). All efforts possible were made to minimize animal suffering.

Production of transgenic mice overexpressing GMF

First, we prepared a construct to create transgenic mice overexpressing GMF (GMF-TG). The transgene construct was prepared by cloning the coding region of GMF (97-915 bp) to a pCAGGS vector [50]. The purified construct was used for microinjection of fertilized oocytes from C57BL6/J mice. The transgenic mice were established at Oriental BioService (Kyoto, Japan) and maintained on a C57BL6/J genetic background. The GMF-TG mice were identified by PCR screening.

Animals and diets

C57BL6/J (wild-type) mice were purchased from Crea Japan Inc. (Tokyo, Japan). The GMF-TG and wild-type male mice were used for the analyses. All of the mice employed in the study were housed in standard cages with 3-4 mice per cage under controlled temperature ($21 \pm 2^{o}C$) and humidity (50%) conditions, with a 12 h light/dark cycle. The mice were given free access to tap water and basal diets (CE-2, Crea-Japan Inc., Tokyo, Japan) throughout the experiments.

The mice were kept until natural death and monitored twice a week for clinical signs, morbidity or mortality during the experimental period of 155 weeks. The clinical signs

used to assess health and welfare were characterized by obvious symptoms, like the moribund state, hypokinesia, fever, severe cachexia, loss of body weight, lack of grooming or nesting, not eating or drinking, alopecia, skin atrophy and spinal curvature [51,52]. Euthanasia was performed by an inhaled anesthetic overdose, followed by sevoflurane (Sevofrane, Maruishi Pharma., Osaka, Japan) in order to minimize animal suffering from distress or pain.

Histological analyses, PCR analyses and Western blot analyses: Tissue samples were obtained after the euthanasia, which was performed by an overdose of the inhaled anesthetics sevoflurane.

PCR screening, hair-growth assay and creatinine levels: The experiments were performed under anesthesia maintained by the inhalation of sevoflurane.

PCR screening

Genomic DNA was extracted from 1-2 mm sections of the tail tip. The DNA was purified using the Wizard SV Genomic DNA Purification System (Promega, Madison, WI), according to the manufacturer's instructions. Briefly, mouse tail was incubated overnight at 55^{o}C with digestion solution master mix, and then added Wizard SV Lysis Buffer. Lysate was transferred to the DNA binding column tube by centrifugation at 13,000 ×g for 3 min at 25^{o}C. For elution of the DNA, the DNA binding filter column was added a 250 μl Nuclease-Free Water. The DNA was eluted by centrifugation at 13,000 ×g for 1 min at 25^{o}C. The PCR screening was carried out using the T3 (5'-AATTAACCCTCACTAAAGGG-3') and T7 (5'-GTAATACGACTCACTATAGGGC-3') primer sequences and TaKaRa Taq (TaKaRa, Shiga, Japan) under the following conditions: 94^{o}C 90 s (1 cycle); 94^{o}C 60 s,

55°C 60 s, 72°C 90 s (35 cycles) in the GeneAmp PCR System 9700 (Life technologies, Carlsbad, CA). The PCR primers employed were obtained from Sigma-Aldrich (St. Louis, MO).

Histological analyses

Mice were sacrificed at 30 weeks for the histological analyses. Tissue sections were fixed in 10% neutral-buffered formalin solution, paraffin embedded, sectioned, and stained with hematoxylin-eosin (HE), periodic acid–schiff (PAS) and masson trichrome (MT), all of which were performed at Applied Medical Research (Osaka, Japan). The sections were examined using an Olympus BX51 microscope & DP70 digital camera system (Olympus, Tokyo, Japan).

Hair-growth assay

Employing age-matched mice, dorsal hair was removed by depilatory cream from a square grid of skin measuring 1.5 cm×1.5 cm. Hair regrowth was scored 15 days later from digital photographs and a semi-quantitative assessment was done using 6-9 hair samples/animal. A square measuring 0.5 cm×0.5 cm was also used for the collection of hair samples.

Creatinine levels

When the mice were 60-80 weeks old, the whole blood samples were collected from the fasting mice by venipuncture from the caudal vein into syringes without anticoagulant, and the serum samples were acquired from the whole blood samples. The serum samples were incubated for 30 min at RT and separated by centrifugation at 3,000 rpm for 15 min at 4°C after cooling with ice. Serum creatinine levels were measured employing the CRE-EN kit (Kainos, Tokyo, Japan).

RNA extraction and reverse transcription for PCR analyses

Total mouse tissue RNA was extracted with TRIzol reagent (Life technologies), according to the manufacturer's instructions, followed by DNase treatment to eliminate contaminating genomic DNA. Briefly, mouse tissue was homogenized in 1 mL of TRIzol reagent. The homogenized sample was added a 200 μl chloroform, and then centrifuged at 12,000 ×g for 15 min at 4^{o}C. The aqueous phase was transferred to a new tube. The RNA pellet was eluted by centrifugation at 12,000 ×g for 10 min at 4^{o}C after adding a 500 μl 100% isopropanol to the aqueous phase. Total mouse tissue RNA was prepared by resuspension of the RNA pellet in RNase-free water, and then eliminated contaminating genomic DNA using Recombinant DNase I (TaKaRa).

Single-stranded DNA was generated from the RNA with random hexamers primers using the Transcriptor First Strand cDNA synthesis kit (Roche, Mannheim, Germany) under the following conditions: 65^{o}C 10 min; 25^{o}C 10 min; 55^{o}C 30 min; 85^{o}C 5 min in the Program Temp Control System PC-708 (ASTEC, Fukuoka, Japan).

Confirmation of gene expression of GMF

Quantitative PCR analyses of the GMF genes were performed with TaqMan Universal PCR Master Mix (Life technologies) and TaqMan probe of GMF and mouse GAPDH under the following conditions: 50^{o}C 2 min (1 cycle); 95^{o}C 10 min (1 cycle); 95^{o}C 15 s, 60^{o}C 1 min (40 cycles) in the 7500 Fast Real-Time PCR System (Life technologies). The TaqMan probe for each GMF and mouse GAPDH employed was obtained from Life technologies. The expression levels of the GMF mRNA were normalized to those of the GAPDH mRNA.

Gene expression of Zmpste24, TGF-β1, CTGF, and p21/waf1

Real-time PCR analyses were performed with SYBR Premix Reagent (TaKaRa) under the following conditions: 95°C 10 s (1 cycle); 95°C 5 s, 60°C 34 s (40 cycles); 95°C 15 s, 60°C 1 min, 95°C 15 s (1 cycle) in the 7500 Fast Real-Time PCR System (Life technologies). The following primer pairs were used for real-time PCR analyses: The GAPDH forward primer sequence 5'-AAATGGTGAAGGTCGGTGTG-3', and its reverse primer sequence 5'-TGAAGGGGTCGTTGATGG-3', The Zmpste24 forward primer sequence 5'-CCTTCAGCTTCTGGTCAGGACTCTA-3', and its reverse primer sequence 5'-CTGGTCCAAAGCCAGCAGAAC-3', The TGF-β1 forward primer sequence 5'-GTGTGGAGCAACATGTGGAACTCTA-3', and its reverse primer sequence 5'-TTGGTTCAGCCACTGCCGTA-3', The CTGF forward primer sequence 5'-ACCCGAGTTACCAATGACAATACC-3', and its reverse primer sequence 5'-CCGCAGAACTTAGCCCTGTATG-3', The p21/waf1 forward primer sequence 5'-CTGTCTTGCACTCTGGTGTCTCA-3', and its reverse primer sequence 5'-CCAATCTGCGCTTGGAGTGA-3'. The PCR primers employed were obtained from TaKaRa. The expression level of each mRNA was normalized to that of the corresponding GAPDH mRNA.

Western Blot Analyses

The total protein obtained from each mouse kidney was extracted with RIPA buffer [53], and protease inhibitor (Roche). A total of 50 μg of each sample was separated by 5-20% polyacrylamide gel and transferred to a nylon membrane (Hybond-P: GE Healthcare, Buckinghamshire, UK). Blots were blocked with 5% ECL Blocking Agent (GE Healthcare) in TBS (25 mM Tris, 137 mM NaCl, 2.7 mM KCl, pH 7.4) plus 0.1%

Tween 20 (Sigma-Aldrich), and incubated overnight at 4^{o}C with 1/400 anti-Lamin A/C polyclonal antibody rabbit (Bio Vision, Milpitas, CA), 1/1,000 p21 monoclonal antibody mouse (#60214-1-Ig, Proteintech, Chicago, IL), or 1/4000 alpha actin polyclonal antibody rabbit (#23660-1-AP, Proteintech). Finally, the blots were incubated with 1/10,000 HRP-linked anti-rabbit IgG or anti-mouse IgG (GE Healthcare). Antibody binding was detected with the ECL Prime chemiluminescence system (GE Healthcare), with subsequent exposure to LAS-3000 chemiluminescence (GE Healthcare). The protein expression of p21/waf1 was assayed employing the western blot method and quantified using Image J densitometry software.

Statistical Analyses

The data analyses were performed using the Kaleida Graph software package (Synergy Software, Tokyo, Japan). Values were expressed as means ± S.E. Statistical analyses for the comparison of two groups were performed using Unpaired Student's *t* test. For the lifespan assessments, data were analyzed employing the Kaplan-Meier method and log-rank test using StatMate'3 software package (ATMS Inc., Tokyo, Japan). *P* values < 0.05 were considered to indicate statistical significance.

2.3 Results

Transgenic mice overexpressing GMF

It is considered that GMF is normally expressed in the brain in a tissue-specific manner [4-6]**.** However, GMF is also induced ectopically in renal proximal tubules by proteinuria [16,17]. In order to analyze the previously unknown roles of GMF overexpression in non-brain tissues, we first created the GMF-TG mice, as described in the 'Materials and Methods' section (Figure 5A). We confirmed that the specific sequence, which was incorporated in a genome, was expressed in the correct direction in established transgenic lines (data not shown). Next, we conducted quantitative PCR analyses to confirm the expression of GMF in the GMF-TG mice. In this study, we used kidney tissue because it has been shown that GMF overexpression was ectopically induced in kidney tissue by proteinuria [16,17]. The results of the quantitative PCR analyses, employing mRNA obtained from the kidneys of the wild-type and GMF-TG mice, showed that GMF mRNA from the GMF-TG mice increased significantly (approximately 7-fold), compared with the wild-type mice (Figure 5B).

Phenotypes of GMF-TG mice

We bred the GMF-TG mice with the wild-type mice. During the breeding period, only GMF-TG mice began to show signs of aging in appearance, including hair graying and lack of hair glossiness, at about the age of 30 weeks (hereafter, 30 weeks, etc.). We investigated whether the GMF-TG mice would develop features of accelerated aging.

Prematurely aged mice exhibit early aging-like appearance phenotypes, including increased hair loss, lordokyphosis of the spine, a shortened lifespan and growth retardation, compared to wild-type mice [54-58]. We monitored the aging-related

phenotypes of the GMF-TG and wild-type mice during an experimental period of 155 weeks. The GMF-TG mice developed alopecia early, by about 75 weeks, while the wild-type mice started to show alopecia after about 100 weeks (Figure 6A-B and Table II). Some GMF-TG mice also exhibited skin atrophy and spinal curvature. These phenotypes were not detected in the wild-type mice (Figure 6 and Table II). We also found that some of the GMF-TG mice died within 60 weeks. The average lifespan of the GMF-TG mice was about 119 weeks, and that of the wild-type mice was about 126 weeks. Kaplan-Meier representations of the survival curves demonstrated that the GMF-TG mice died significantly earlier than the wild-type mice (Figure 7). There was no statistically significant difference in the body weight and size in mature-adult mice (at about 20 weeks) (data not shown).

Next, we examined aging-related changes in the tissue structure. Degenerative changes in skin tissue are readily visible, so they can be detected easily [57]. Decreased hair regrowth has often been reported in prematurely aged mice [55-57]. Because hair growth assays can be employed to monitor degenerative changes without adversely affecting the mice, we employed them to investigate the influence of aging on skin tissue. When dorsal segments of skin were shaved on age-matched mice, the GMF-TG mice showed sparse hair regrowth after 15-days. In contrast, at the same age, the wild-type mice displayed robust hair regrowth (Figure 8A-C). The hair regrowth ratio significantly declined in the GMF-TG mice at 10, 60 and 80 weeks, compared with the wild-type mice at the same age (Figure 8D). In the kidney, liver, and abdominal aorta at 30 weeks, there were no histologically detectable changes between the GMF-TG and wild-type mice, as indicated in Figure 9. These results suggested that the GMF-TG mice

developed mild premature aging phenotypes.

HGPS is associated with premature alopecia, which is one of the well-known premature-aging syndromes due to laminopathies, seen in humans [44]. Cells and tissue from HGPS patients exhibited an accumulation of abnormal lamin A (progerin) [46,47]. The phenotypes characterized in the skin of the GMF-TG mice, such as alopecia and skin atrophy, seemed to be similar to that of laminopathy-based premature aging (Figure 10). Therefore, we hypothesized that an accumulation of abnormal lamin A resulted in the accelerated aging phenotypes shown in the GMF-TG mice. In order to analyze the abnormalities of the lamin A in the tissue of the GMF-TG mice, we examined the lamin A protein in the kidney by western blotting. At 10 weeks of age, no lamin A abnormalities were exhibited in the kidney of either the GMF-TG or wild-type mice (Figure 11A). However, at 60 weeks of age, an accumulation of abnormal lamin A (prelamin A) was detected in the kidneys of the GMF-TG mice, but not in the wild-type mice (Figure 11B). Next, we evaluated the expression levels of the cleaving enzyme of prelamin A (*Zmpste24*) gene in the kidneys by real-time PCR analyses to confirm the mechanism of the accumulation of prelamin A. At 10 weeks of age, the expression of Zmpste24 mRNA tended to decrease in the GMF-TG mice (Figure 11C). At 60 weeks of age, a significant decrease was demonstrated in the expression of Zmpste24 mRNA in the GMF-TG mice, compared with the wild-type mice at the same age (Figure 11D). These results demonstrated that the GMF-TG mice exhibited an accumulation of prelamin A, accompanied by a reduction of *Zmpste24* gene expression in the kidney tissue. On the basis of these results, we investigated the degree of aging in the kidney

tissue of the GMF-TG mice. In the kidney, aging-associated changes are characterized by structural changes, including glomerulosclerosis and interstitial fibrosis [59,60], as well as the decline of renal function [60]. It has been suggested that the transforming growth factor-β1 (*TGF-β1*) gene is one of the factors that promote the process of renal interstitial fibrosis associated with aging [59]. The connective tissue growing factor (*CTGF*) gene is known as a downstream mediator of TGF-β1. In order to investigate age-associated changes in the kidneys, we evaluated the expression levels of the *TGF-β1* and *CTGF* genes by real-time PCR analyses. In the kidney tissue of the GMF-TG mice at 10 weeks of age, the expression of TGF-β1 mRNA increased significantly, compared with the wild-type mice (Figure 12A). However, there was no statistically significant difference between the expression of CTGF mRNA of the kidney of the GMF-TG and wild-type mice at 10 weeks of age (Figure 12B). Importantly, in the GMF-TG mice at 60 weeks of age, the expression of both TGF-β1 and CTGF mRNA in the kidney increased significantly, compared with that of the wild-type mice (Figure 12C and D). It has been reported that serum creatinine was increased in old mice compared with young mice, suggesting the decline of renal function with advancing age [60]. Figure 13 showed that serum creatinine was increased in the old GMF-TG mice (Average age: 72.8 weeks of age) compared with the old wild-type mice (Average age: 84.8 weeks of age). These results demonstrated that the GMF-TG mice showed premature-aging phenotypes in the kidney tissue, probably through an accumulation of prelamin A. These findings suggested that the GMF-TG mice might show a tendency for laminopathy-based premature aging.

The mechanisms of laminopathy-based premature aging in the GMF-TG mice

We attempted to demonstrate the mechanisms of laminopathy-based premature aging in the GMF-TG mice. It has been suggested that premature aging in laminopathy model mice is linked to p53 pathway activation [61]. The activated p53 pathway induces cell/tissue senescence and eventually leads to accelerated aging [23,24]. We examined whether the expression of *p21/waf1* gene, a p53 downstream target gene, would increase in the kidneys of the GMF-TG mice at 10 and 60 weeks of age, and found that the expression of p21/waf1 mRNA and protein at 10 weeks increased significantly, compared with the wild-type mice (Figure 14A and C). However, at 60 weeks, a significant decrease in the expression of p21/waf1 mRNA was demonstrated in the GMF-TG mice, compared with the wild-type mice at the same age (Figure 14B). There was no statistically significant difference between protein expression of p21/waf1 in the kidney of the GMF-TG and wild-type mice at 60 weeks (Figure 14C). These results suggested that the p53 pathway was activated only at an earlier age in the GMF-TG mice, or that some compensative responses might be activated during a later stage in these mice.

2.4 Discussion

In order to examine the roles of GMF overexpression in non-brain tissues *in vivo*, a novel line of mice, GMF-TG mice, was established in this study (Figure 5). We first found that the GMF-TG mice exhibited a premature onset of aging-associated symptoms seen in physiological human aging, including a lack of hair glossiness, hair graying, alopecia, skin atrophy, and curvature of the spine (Figure 6 and Table II). We hypothesized that GMF overexpression in non-brain tissues *in vivo* might play role in aging. Our findings demonstrated that the GMF-TG mice had short lifespans (Figure 7) and showed premature degenerative changes in skin tissue (e.g., reduced hair regrowth) (Figure 8). However there were no visible age-related histological changes in the kidney, liver, and abdominal aorta (Figure 9).

Mutations or altered post-translational lamin A processing lead to an accumulation of lamin A abnormalities, such as progerin or prelamin A [42]. Because these nuclear intermediate filaments, such as lamin A/C, function as a mesh to protect the nucleus from mechanical stress, the alteration of lamin A protein causes a loss of nuclear stability and integrity, manifesting premature-aging syndromes (e.g., HGPS) [40-43]. The GMF-TG mice were characterized by changes in appearance, such as alopecia and skin atrophy from an earlier stage of life (Figure 6 and Table II). In appearance, these phenotypes were similar to those seen in laminopathy-based premature aging (Figure 10). In this study, we investigated whether or not the accelerated aging phenotypes that were observed in the GMF-TG mice were associated with laminopathies. First, we found that the GMF-TG mice accumulated an abnormal lamin A (prelamin A) with age in the kidney tissue (Figure 11A and B). Second, we demonstrated that the GMF-TG

mice showed a reduced expression of the cleaving enzyme of prelamin A (Zmpste24) in the kidney tissue, from an earlier stage of life (Figure 11C and D), suggesting that the GMF-TG mice would probably be affected by secondary laminopathy [42] due to an accumulation of prelamin A, accompanied by a reduction in the expression of Zmpste24. Finally, we confirmed the increased *TGF-β1* and *CTGF* gene expression and the decline of renal function (e.g. increased serum creatinine) (Figure 12-13). The GMF-TG mice exhibited premature-aging phenotypes in the kidney tissue. The results of the present study suggest that the GMF-TG mice might develop accelerated aging phenotypes due to secondary laminopathy.

As animal models employed in studies on secondary laminopathies, Zmpste24-knockout mice (Zmpste24-/- mice) are well-known [62]. Zmpste24-/- mice exclusively produce prelamin A as a consequence of Zmpste24 deficiency [62]. These mice exhibit severe phenotypes consistent with human laminopathies (e.g. HGPS and restrictive dermopathy), including growth retardation, jaw and bone abnormalities, alopecia and shorter lifespan [62]. Intriguingly, the GMF-TG mice exhibited phenotypes without the severe ones, such as growth retardation or extremely short lifespan during the study (Figure 6-7 and Table II). Comparing to secondary laminopathies caused by genetic mutation, the severity of the phenotypes observed in the GMF-TG mice was very mild. In regard to the contribution of prelamin A accumulation to the pathological aging phenotypes, several studies were conducted using Zmpste24-/- mice and Zmpste24-/- Lmna+/- mice [61,63]. The accumulation levels of prelamin A of the Zmpste24-/- Lmna+/- mice were significantly reduced, compared to that of Zmpste24-/-

mice [61,63]. In response to this prelamin A reduction, the phenotypes observed in the Zmpste24-/- mice were largely rescued in the Zmpste24-/- Lmna+/- mice [61,63]. Moreover, there were no differences shown in the body size, weight or lifespan between the Zmpste24-/- Lmna+/- mice and the wild-type mice during the studies [61]. These results suggested that the levels of accumulation of prelamin A might at least partially contribute to the phenotypes seen in the Zmpste24-/- mice, but that is not only the critical determinant for the aging phenotype and the precise underlying pathogenic mechanisms still need to be explored [61,63]. We detected an accumulation of prelamin A only in the old GMF-TG mice (Figure 11A and B). The young GMF-TG mice tended to show a reduced expression of the *Zmpste24* gene (Figure 11C). It is conceivable that the amount of prelamin A in the GMF-TG mice might be less than that found in the mouse models employed for secondary laminopathies. Here, we propose that the characteristic of the mild phenotypes shown in the GMF-TG mice might be because of the slowly increased pattern of expression time course and/or the expression amount of prelamin A.

Several studies showed that the presence of lamin A abnormalities, such as progerin or prelamin A, was detected in normal human aging [46-49]. Furthermore, an accumulation of prelamin A in healthy aging was associated with the down-regulation of Zmpste24 [48,49]. However, at present, the molecular mechanisms that regulate the expression of Zmpste24 have not been fully clarified. Recent studies showed that the gene expression of Zmpste24 was reduced in response to oxidative stress [48,49]. Here, we can speculate that the induction of GMF in non-brain tissues might cause an

oxidative stress-related reduction of Zmpste24, presumably due to its vulnerability to oxidative stress [18]. We believe that GMF overexpression in local tissue might contribute to the promotion of the local aging process by causing secondary laminopathy. GMF is ectopically induced by proteinuria in renal tubules [16,17]. CKD associated with proteinuria might accelerate the regular aging process in kidney tissue and also enhance the progression of CKD, which consequently might have an impact on systemic pathological changes, including organismal aging, cardiovascular damage and inflammatory changes.

Several *in vivo* studies have demonstrated that senescent cells accumulate with age [23]. Senescence is considered to be related to organismal aging, through the disruption of tissue functions [23,24,64,65]. Senescence is regulated by the p53 or p16-Rb pathway, both of which are activated in the presence of oxidative stress [23,24]. Some studies have demonstrated that an accumulation of prelamin A induces a significant increase in senescence-associated biomarkers, such as SA-β-gal staining [48,61]. This suggests that the reduction of Zmpste24 levels and the accumulation of prelamin A might be linked to the activation of the p53 pathway [61], leading to senescence and premature aging [23,24]. On the other hand, Kudlow et al. [66] reported that the expression of p53 target genes was not highly up-regulated in laminopathy cases. Varela et al. [61] examined whether or not the absence of p53 could result in a recovery of the premature-aging phenotypes that were observed in the laminopathy model mice. Zmpste24-/- p53-/- mice exhibit a gain in weight and an increased lifespan, compared with Zmpste24-/- mice [61]. The expression of p53 target genes, such as the *p21/waf1* gene, decreased in

Zmpste24-/- p53-/- mice, compared with age-matched Zmpste24-/- mice [61]. In Zmpste24-/- p53-/- mice, the phenotypes seen in the Zmpste24-/- mice were partially improved by the absence of the *p53* gene [61]. These findings indicate that the activation of the p53 pathway might play a role in the progression of aging in laminopathy cases.

In the present study, the expression of p21/waf1 mRNA and protein increased in the GMF-TG mice at 10 weeks of age (Figure 14A and C), suggesting that premature aging in the young GMF-TG mice might be associated with the p53 pathway. To our surprise, the GMF-TG mice showed a reduced expression of p21/waf1 mRNA at 60 weeks of age (Figure 14B). There was no change in the expression of the p21/waf1 protein (Figure 14C). Because the p21/waf1 is a key mediator of the p53-dependent cell cycle arrest and senescence process, the expression of p21/waf1 is exquisitely regulated by transcriptional, post-transcriptional and post-translational mechanisms [67]. We can speculate that the regulatory factors of the p21/waf1 might be influential in the old GMF-TG mice in order to modulate p53-dependent senescence. For example, the p400 E1A-associated protein, which inhibits p53-dependent p21/waf1 transcription [68], modulates cell fate decisions (cell cycle progression, apoptosis, or senescence) by the ROS homeostasis [69]. It is conceivable that the up-regulation of p400 might be induced in the later age of GMF-TG mice in order to modulate increased oxidative stress caused by the overexpressed GMF in non-brain cells [18]. Further studies are required to elucidate these issues.

In summary, we demonstrated that the GMF-TG mice showed very mild accelerated

aging phenotypes, due to secondary laminopathy. In regard to the mechanisms involved in this process, we propose that the ectopic GMF overexpression induces an oxidative stress-related reduction of Zmpste24. This might be associated with the activation of the p53 signaling-pathway, leading to senescence in cells and tissues.

Chapter 3.

Concluding remarks

Lamin A, a component of the nuclear lamina, is spliced products of the *LMNA* gene that is synthesized as a precursor prelamin A [39,42]. Zmpste24, a zinc metalloproteinase, is involved in the maturation of lamin A [39,42]. Mutations in the *LMNA* or *Zmpste24* gene produce mutant lamin A proteins, such as progerin or prelamin A, respectively [42]. The abnormal lamin A has been identified as the cause of laminopathies which are characterized by premature aging [42]. Interestingly, the *Zmpste24* gene expression has been shown to be decreased in response to oxidative stress [48,49]. It suggests that the prelamin A accumulation might be not only caused by genetic mutation, but also by stress signals, such as oxidative stress.

In this study, we identified an accumulation of prelamin A in the GMF-TG mice. It suggests that accelerated aging phenotypes in the GMF-TG mice might be associated with secondary laminopathy, caused by Zmpste24 down-regulation. We propose that GMF overexpression in non-brain tissues could cause down-regulation of Zmpste24 mRNA by through enhancing oxidative injuries due to its vulnerability to oxidative stress (Figure 15) [18]. It is generally recognized that oxidative stress is one of the major factors that promote the aging process in organisms [23,24]. The novel premature aging model mice, the GMF-TG mice, may be useful to understanding molecular mechanisms of aging, and then applicable to anti-aging study.

Figures and Tables

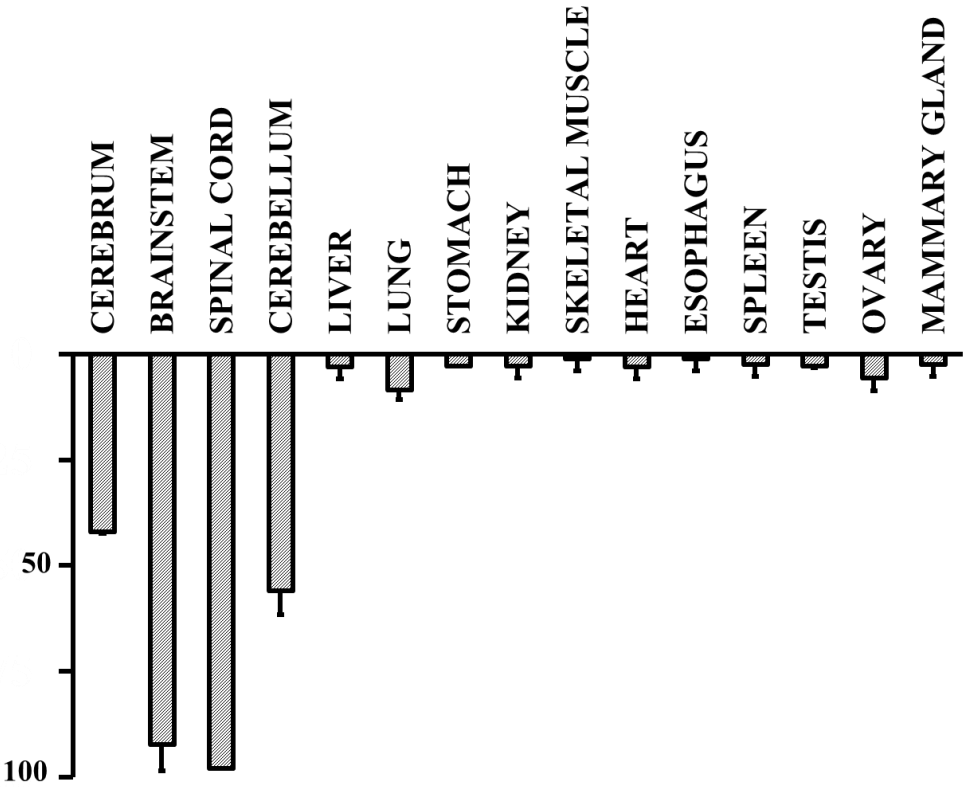

(Zaheer *et al.*, *J Neurochem*, 1993, Figure2)

Figure 1. The expression of GMF mRNA in rat organs at 3 months of age [6].

The expression of glia maturation factor-β (GMF) is predominantly expressed in the nervous system. Low levels of GMF mRNA 10-40 fold less than that in the brain.

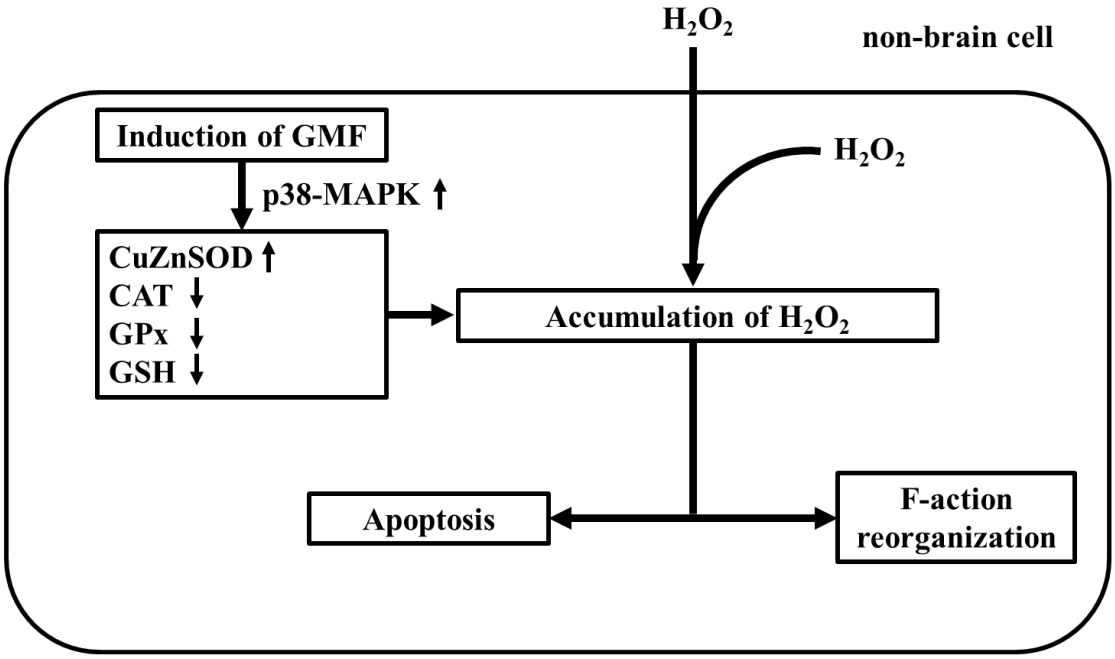

(Modified from Kaimori *et al.*, *J Bio Chem*, 2003, Figure9)

Figure 2. Schematic representation of the effect of GMF overexpression on non-brain cells [18].

GMF overexpression in non-brain cells causes an increase in the activity of the H_2O_2-producing enzyme; copper/zinc-superoxide dismutase (CuZnSOD), a decrease in the activities of the H_2O_2-reducing enzymes; catalase (CAT) and glutathione peroxidase (GPx), and a depletion of the content of the cellular glutathione peroxidase substrate glutathione (GSH) through the p38-MAPK. It promotes a sustained increase in intracellular H_2O_2, leading to F-actin reorganization and apoptosis.

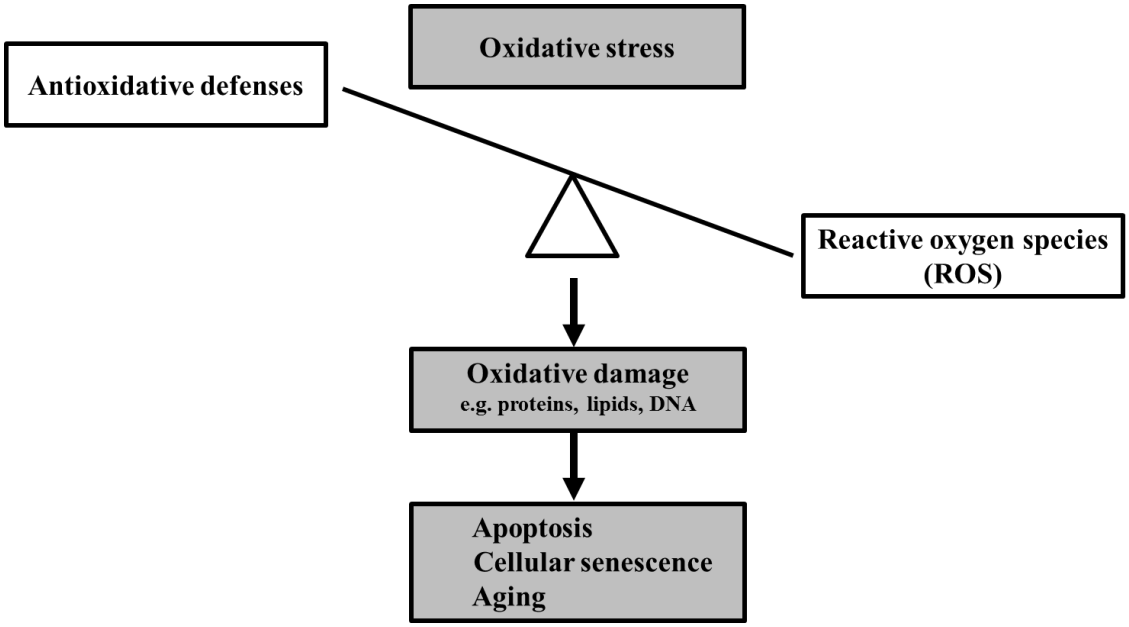

(Modified from Poljsak *et al., Oxid Med Cell Longev*, 2013, Figure2 and Scheme2)

Figure 3. The illustration of relationship between ROS production and the cellular antioxidant defense system and the effects of oxidative stress [21].

Reactive oxygen species (ROS) including singlet oxygen ($^1O_2$), hydrogen peroxide (H_2O_2), superoxide anion radical ($O2\cdot^-$) and hydroxyl radical (·OH) are a byproduct of the normal metabolism of oxygen [20,22]. Oxidative stress results from an imbalance between ROS production and the cellular antioxidant defense system, such as superoxide dismutase (SOD), CAT, GPx and GSH [20,21]. Oxidative stress induces oxidative damage to proteins, lipids and DNA, resulting in apoptosis, cellular senescence and aging [21,23,24].

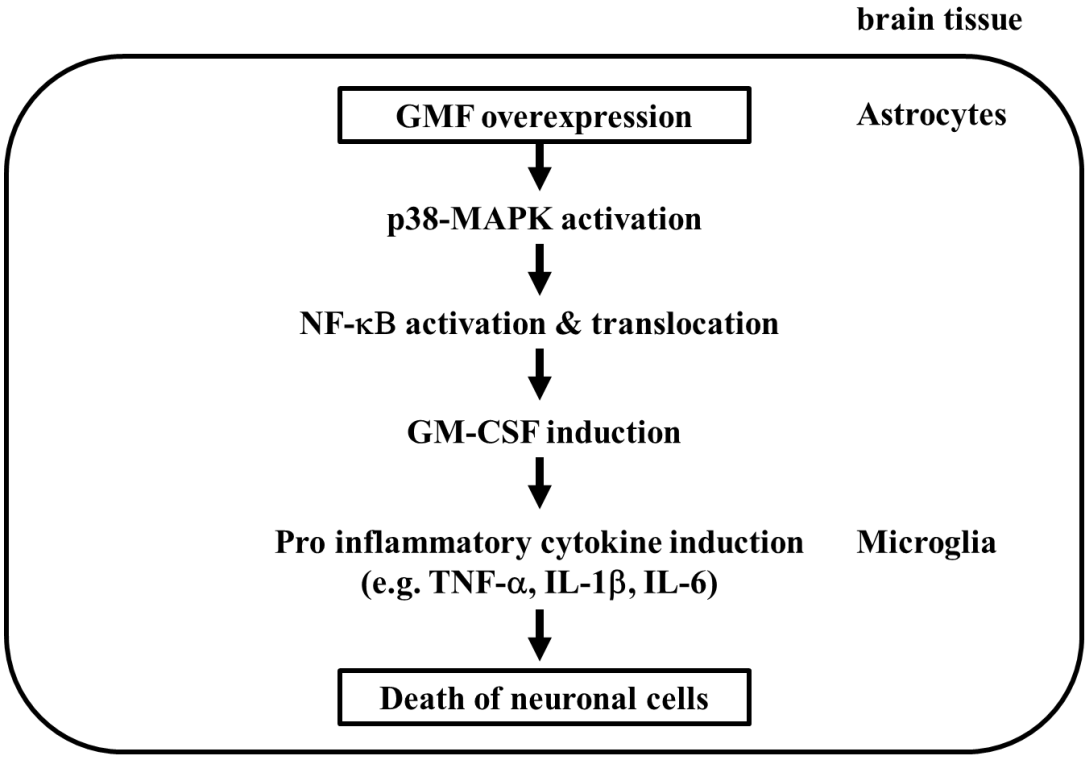

(Modified from Zaherr *et al.*, *J. Neurochem.*, 2007, Figure10)

Figure 4. Hypothetical sequence of events following GMF overexpression in brain tissue by Zaheer et al. [4].

GMF overexpression in brain tissue leads to induction of granulocyte-macrophage colony-stimulating factor (GM-CSF) through p38-MAPK and NF-κB-mediated pathway. GMF-dependent induction of GM-CSF activates microglia to produce TNF-α, IL-1B, IL-6, and IP-10 and that finally results in the death of neuronal cells.

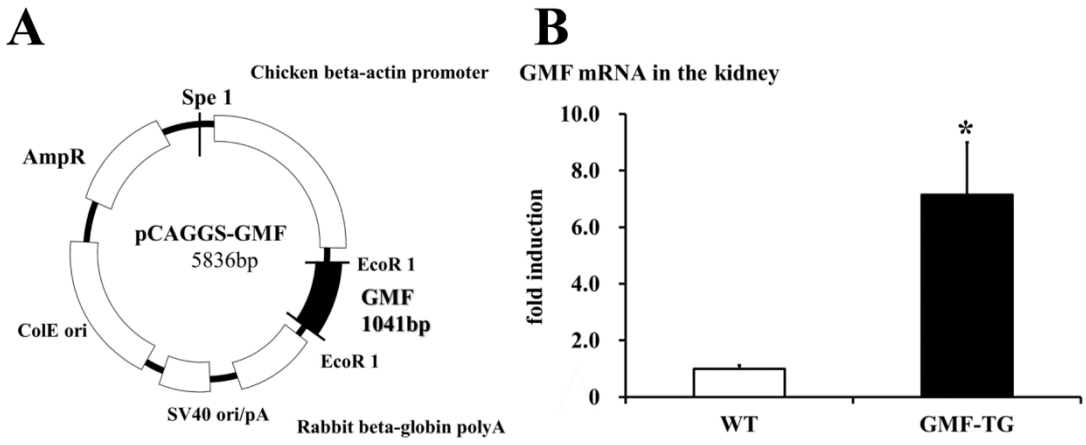

Figure 5. Preparation of transgenic mice overexpressing GMF (GMF-TG).

(A) This figure shows the construct used to prepare the transgenic mice. The construct was prepared by cloning the coding region of GMF (97-915 bp) in a pCAGGS vector. (B) This figure shows that the gene expression of GMF in the kidney of the GMF-TG mice was significantly higher (about 7-fold) than that of C57BL6/J (WT) mice. The data is shown as means ± S.E. (WT; n=3, GMF-TG; n=3). *; $P < 0.05$ vs. WT mice.

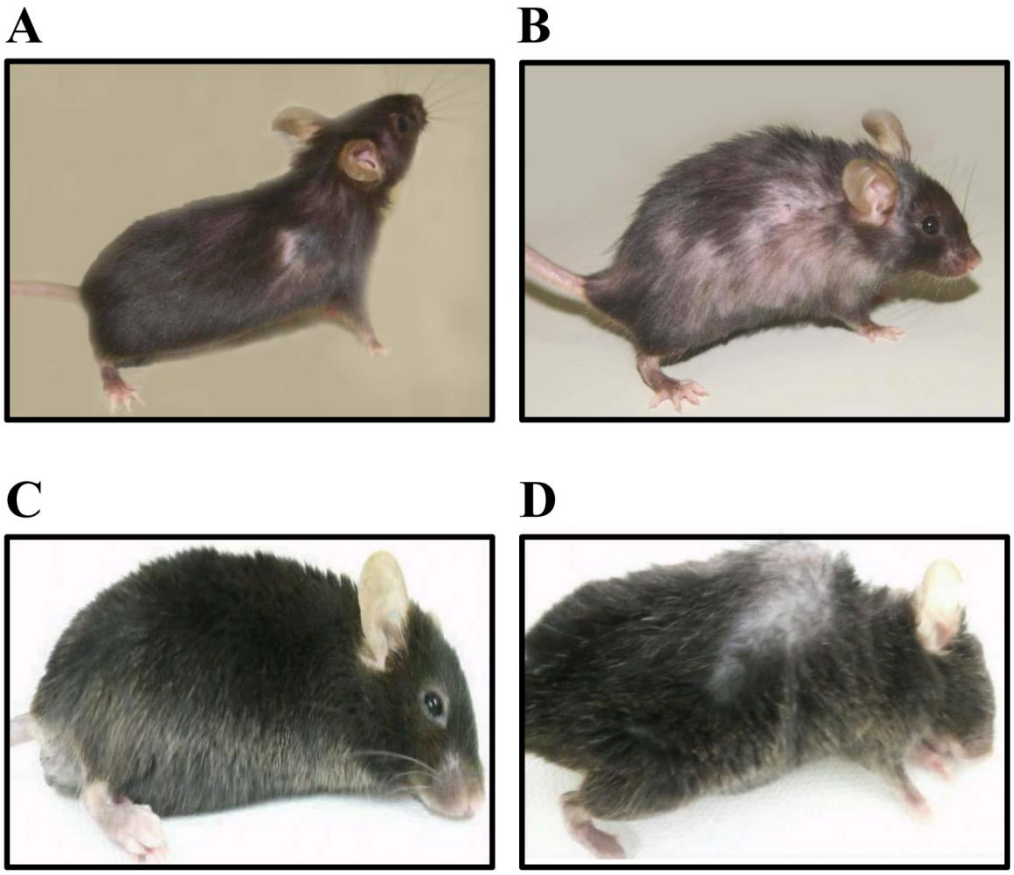

Figure 6. Photograph of WT and GMF-TG mice.

(A-B) These photographs show the representative appearance of the WT (A) and GMF-TG (B) mice at 80 weeks, respectively. The GMF-TG mice showed alopecia and skin atrophy. These phenotypes were not detected in the aged-matched WT mice. (C-D) Indicators of aging phenotypes, such as spinal curvature, were detected in the GMF-TG (D) mice, but not in the WT (C) mice at 110 weeks.

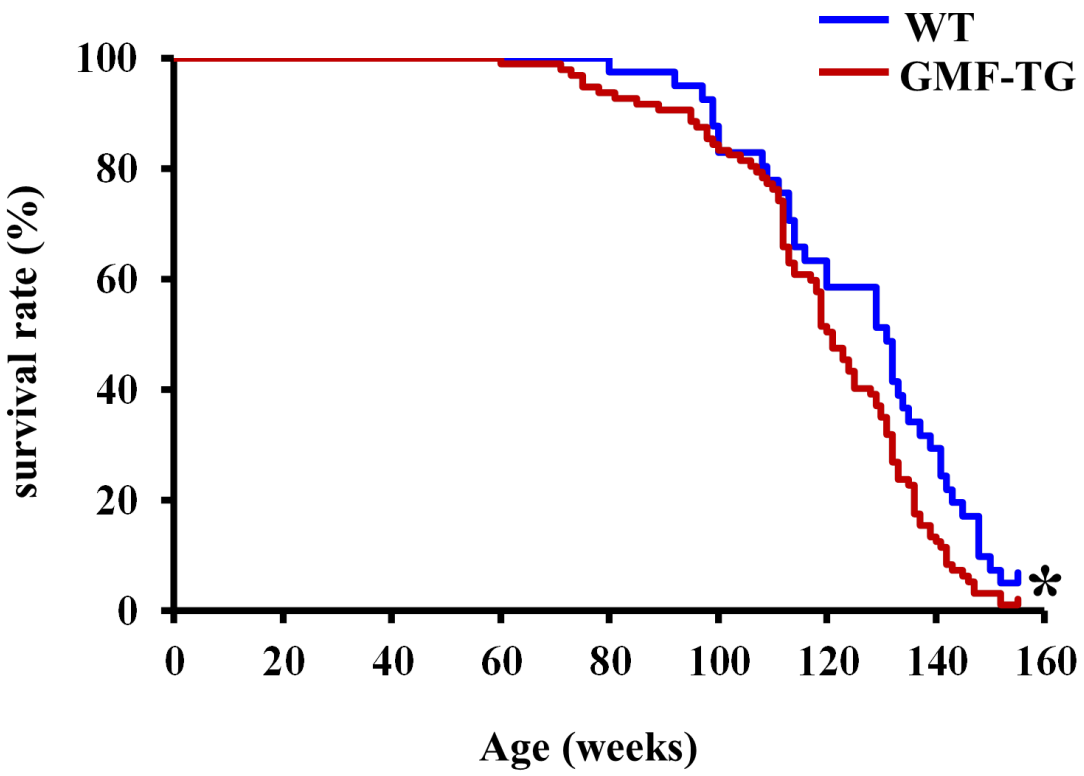

Figure 7. Kaplan-Meier graph of WT and GMF-TG mice.

This figure shows a Kaplan-Meier representation of the survival curves, which revealed that the GMF-TG mice died significantly earlier than the WT mice. The GMF-TG mouse and the two WT mice were alive when the data analysis was performed. None of the mice exhibited any signs of distress or pain due to the clinical symptoms used to assess health and welfare. (WT; n=41, GMF-TG; n=97). *$P < 0.05$ GMF-TG mice vs. WT mice.

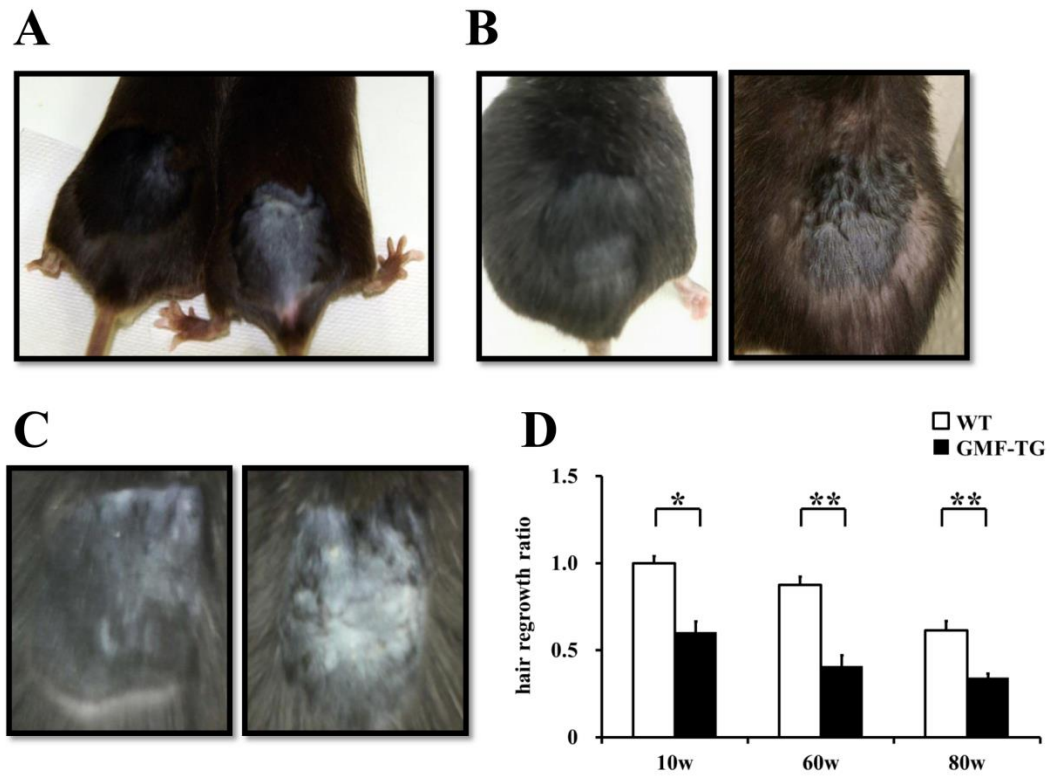

Figure 8. Hair regrowth phenotypes in WT and GMF-TG mice.

(A-C) These photographs show the representative appearance of the WT (A-C; Left) and GMF-TG (A-C; Right) mice at 10 (A), 60 (B) and 80 (C) weeks, 15 days after shaving. Almost no hair regrowth was observed in the GMF-TG mice, whereas the WT mice displayed robust hair regrowth. (D) The figure shows the results for the hair regrowth ratio in the WT and GMF-TG mice at 10, 60 and 80 weeks, 15 days after shaving. The hair regrowth ratio for the GMF-TG mice declined significantly, compared with the WT mice at the same age. The mean of the hair regrowth results for the 10w WT mice is shown as 1. The data is shown as means ± S.E. (10, 60, 80w WT; n=3, 10w GMF-TG; n=6, 60, 80w GMF-TG; n=5). *; $P < .0005$ GMF-TG mice vs. WT mice. **; $P < .0001$ GMF-TG mice vs. WT mice

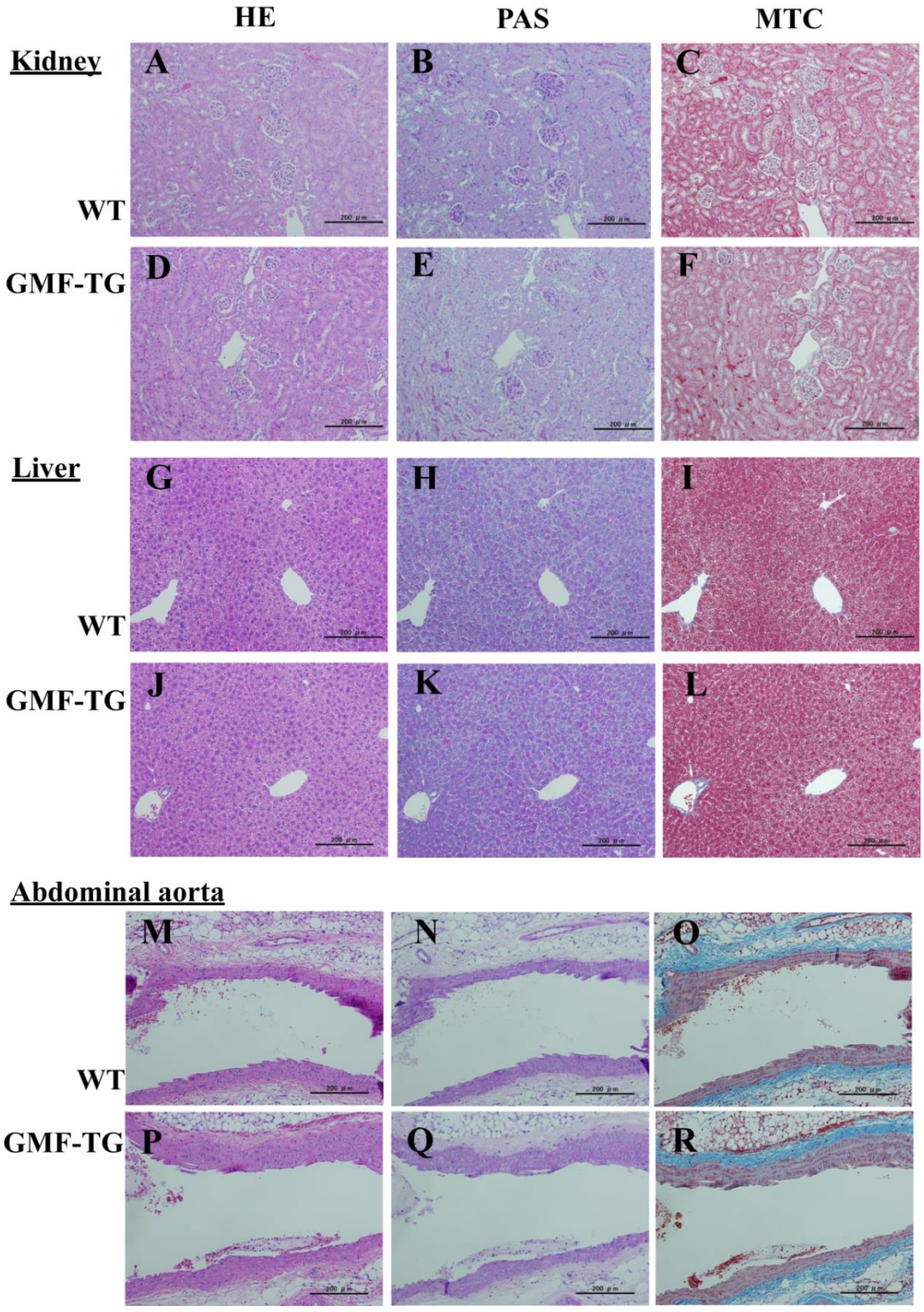

Figure 9. Histological appearance of the kidney, liver and abdominal aorta in WT and GMF-TG mice.

(A-F) These photographs show an overview of the hematoxylin-eosin (HE) (A and D), periodic acid–schiff (PAS) (B and E), and Masson trichrome (MTC) (C and F) stained kidney sections in the WT (A-C) and GMF-TG (D-F) mice at 30 weeks. (G-L) These photographs show an overview of the HE (G and J), PAS (H and K), and MTC (I and L) stained liver sections in the WT (G-I) and GMF-TG (J-L) mice at 30 weeks. (M-R) These photographs show an overview of the HE (M and P), PAS (N and Q), and MTC (O and R) stained abdominal aorta sections in the WT (M-O) and GMF-TG (P-R) mice at 30 weeks. These findings revealed no histological differences between the WT and GMF-TG mice. Magnifications: ×100, Scale Bar = 200 μm.

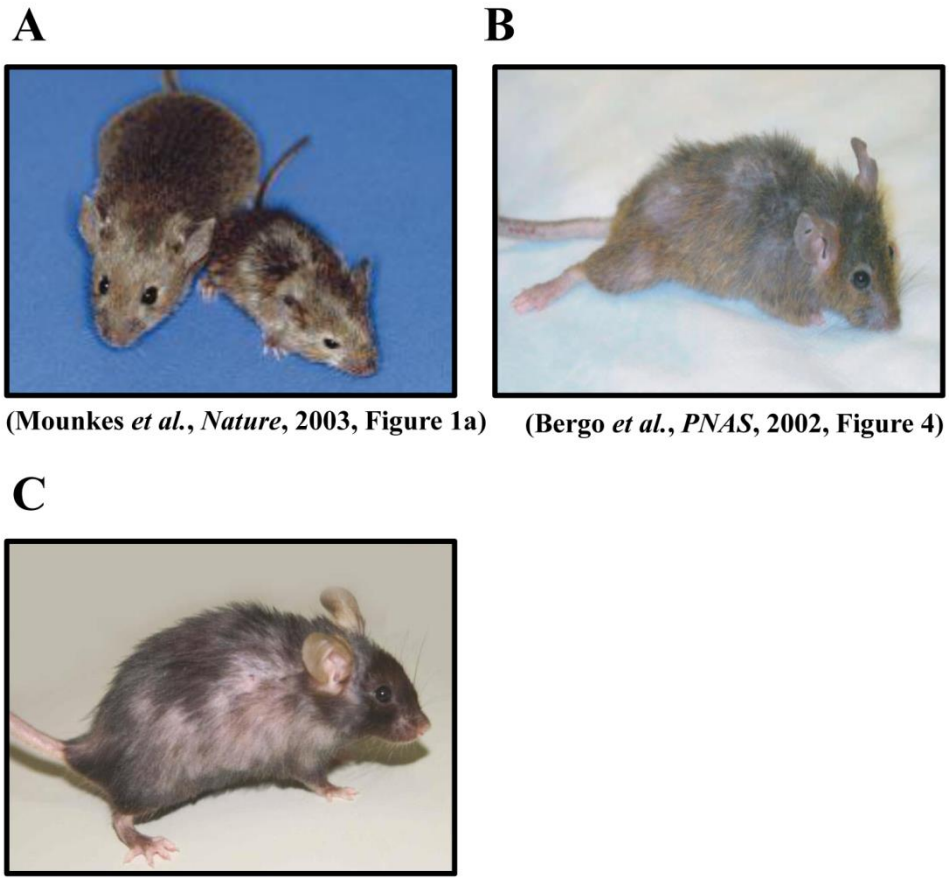

Figure 10. Photograph of mouse models of laminopathies [54,70] and GMF-TG mice.

(A) This photograph shows the representative appearance of mouse models of laminopathies, Lmna $^{L530P/L530P}$ mice (Right) and wild-type mice (Left) [54]. (B) This photograph shows the representative appearance of mouse models of laminopathies, Zmpste24-/- mice [70]. (C) This photograph shows the representative appearance of the GMF-TG mice at 80 weeks. The appearance of the GMF-TG mice, such as alopecia and skin atrophy, seemed to be similar to that of mouse models of laminopathies.

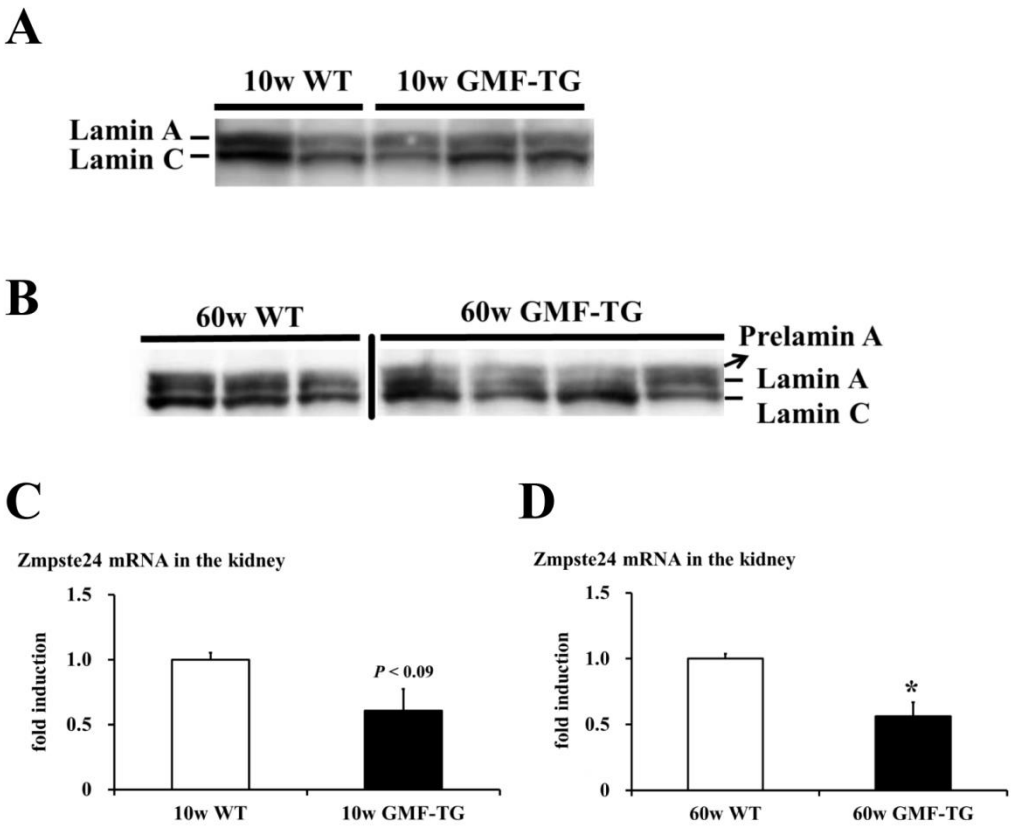

Figure 11. Western blot of lamin A/C and the expression of Zmpste24 in WT and GMF-TG mice.

(A-B) These figures show the results from western blot analyses of the lamin A/C protein in the kidney of the WT and GMF-TG mice at 10 and 60 weeks. Prelamin A was absent in the WT mice at 10 and 60 weeks (A-B; Left) and the GMF-TG mice at 10 weeks (A; Right), but it was detectable in the GMF-TG mice at 60 weeks (B; Right). There were no significant differences between the lamin C protein levels in the WT and GMF-TG mice, confirming equal loading. (C) The expression of Zmpste24 mRNA tended to decrease in the kidneys of the GMF-TG mice at 10 weeks, compared with the WT mice. The data is shown as means ± S.E. (10w WT; n=3, 10w GMF-TG; n=3). $P <$

0.09 vs. 10w WT mice. (D) The expression of Zmpste24 mRNA decreased in the kidneys of the GMF-TG mice at 60 weeks, compared with the WT mice. The data is shown as means ± S.E. (60w WT; n=4, 60w GMF-TG; n=4). *; $P < 0.01$ vs. 60w WT mice.

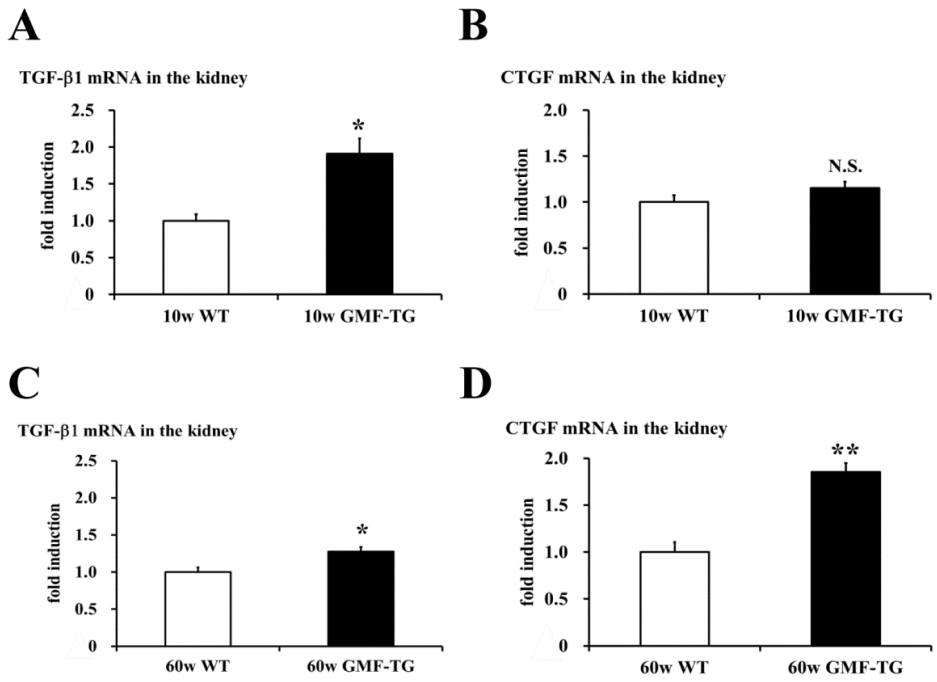

Figure 12. The expression of TGF-β1 and CTGF in WT and GMF-TG mice.

(A-B) The expression of transforming growth factor-β1 (TGF-β1) (A) mRNA increased in the kidneys of the GMF-TG mice at 10 weeks, compared with the WT mice. However, no significant differences were shown in the expression of connective tissue growing factor (CTGF) (B) mRNA in the kidney of the GMF-TG mice at 10 weeks, compared with the WT mice. TGF-β1; The data is shown as means ± S.E. (10w WT; n=4, 10w GMF-TG; n=5). CTGF; The data is shown as means ± S.E. (10w WT; n=3, 10w GMF-TG; n=4). *; $P < 0.01$ vs. 10w WT mice. N.S.; not significant versus 10w WT mice. (C-D) These figures demonstrated a significant increase in TGF-β1 (C) and CTGF (D) mRNA in the kidneys of the GMF-TG mice at 60 weeks, compared with the WT mice at the same age. The data is shown as means ± S.E. (60w WT; n=4, 60w GMF-TG; n=4. *; $P < 0.05$ vs. 60w WT mice. **; $P < 0.001$ vs. 60w WT mice.

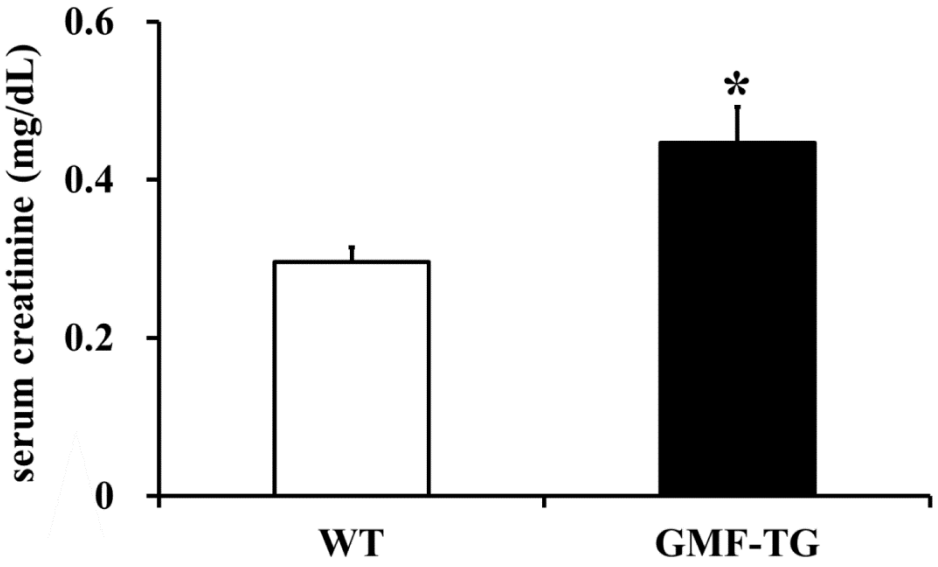

Figure 13. The serum creatinine levels in WT and GMF-TG mice.

This figure shows the result of the serum creatinine levels in the WT and GMF-TG mice, which revealed that serum creatinine was increased in the GMF-TG mice, compared with the WT mice. The data is shown as means ± S.E. (WT; n=4, average age; 84.8 ± 0.25 weeks, GMF-TG; n=4 average age; 72.8 ± 6.24 weeks). *; $P < 0.05$ vs. WT mice.

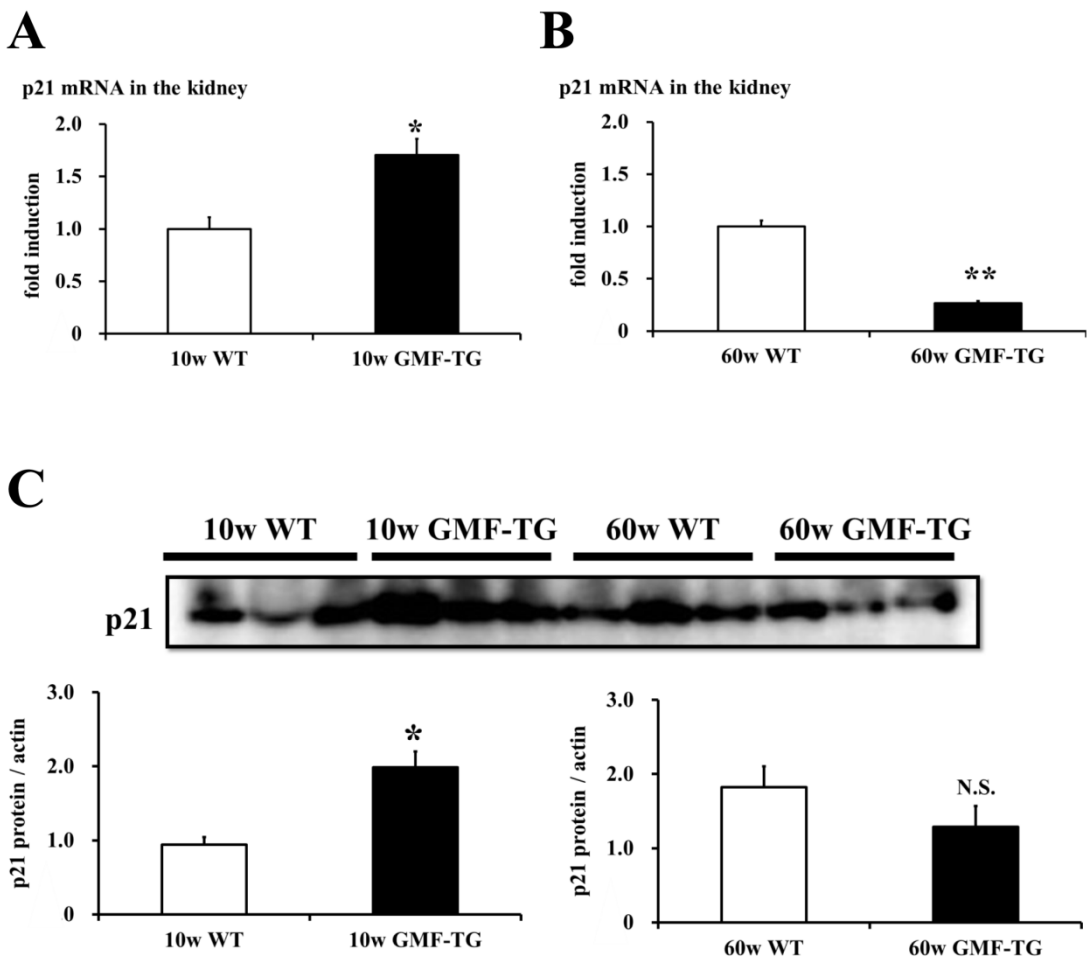

Figure 14. The expression of p21/waf1 mRNA and protein in WT and GMF-TG mice.

(A) The expression of p21/waf1 mRNA increased in the kidneys of the GMF-TG mice at 10 weeks, compared with the WT mice. The data is shown as means ± S.E. (10w WT; n=3, 10w GMF-TG; n=4). *; $P < 0.05$ vs. 10w WT mice. (B) In the kidneys at 60 weeks, the expression of p21/waf1 mRNA in the GMF-TG mice was reduced significantly, compared to that of the WT mice at the same age. The data is shown as means ± S.E.

(60w WT; n=4, 60w GMF-TG; n=4). **; $P < 0.01$ vs. 60 w WT mice. (C) This figure shows the results from western blot analyses of the p21/waf1 protein in the kidney of the WT and GMF-TG mice at 10 and 60 weeks. The data shown is representative data on the estimated ratios of p21/waf1 to α-actin, in the case of equivalent protein loading within a gel. Increased p21/waf1 protein levels were detected in the GMF-TG mice at 10 weeks, compared with the WT mice. However, there was no difference in the levels of p21/waf1 protein between the GMF-TG and WT mice at 60 weeks. The data is shown as means ± S.E. (10, 60w WT; n=3, 10, 60w GMF-TG; n=3). *; $P < 0.05$ vs. 10w WT mice. N.S.; not significant versus 60w WT mice.

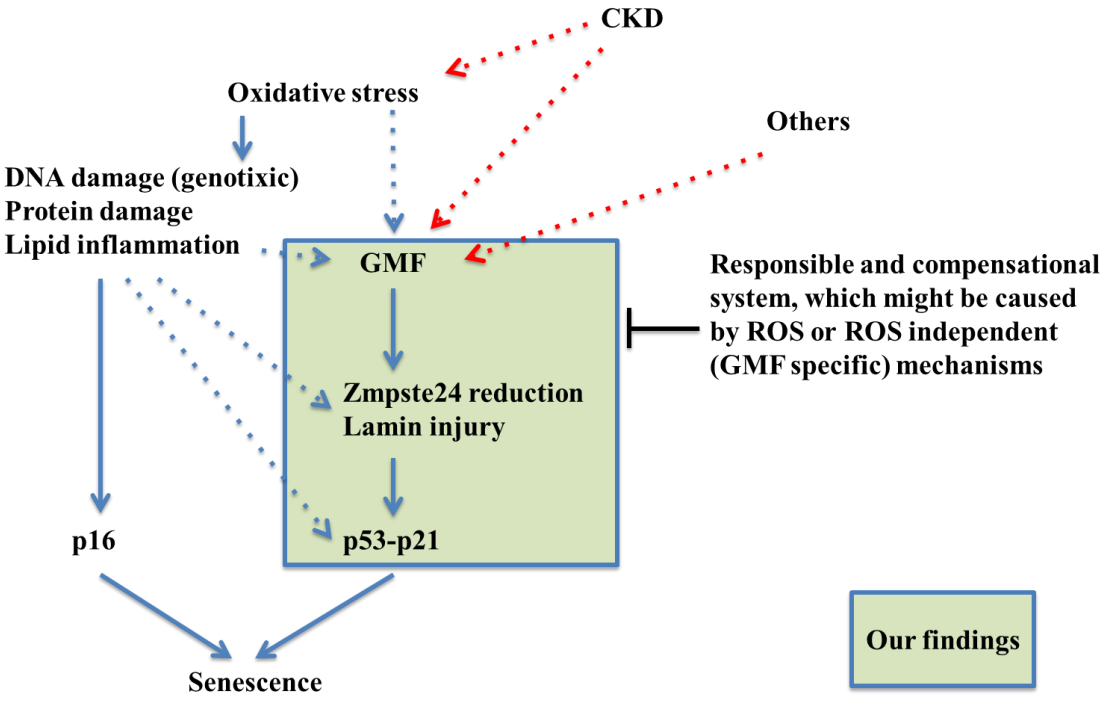

Figure 15. Hypothetical schematic representation of the novel role of GMF overexpression in non-brain tissues *in vivo*.

This study showed that the GMF-TG mice developed very mild accelerated aging phenotypes due to lamin injury caused by Zmpste24 down-regulation. Zmpste24 is down-regulated in response to oxidative stress [48,49], which appears to be associated with the activation of p53 and p16-Rb pathways [48]. Oxidative stress activates the p53 and p16-Rb pathways, inducing senescence and eventually leading to accelerated aging [23,24]. It is conceivable that the ectopic GMF overexpression might be a factor connecting aging and lamin injury through oxidative stress.

Table I. Definition of chronic kidney disease [25].

Chronic kidney disease is diagnosed according to the criteria listed as follows.

Criteria for chronic kidney disease (CKD): (either of the following present for > 3 months)	
Markers of kidney damage (one or more)	**Albuminuria (albumin excretion rate (AER) ≥ 30mg/24 hours; albumin creatinine ratio (ACR) ≥ 30 mg/g [≥ 3 mg/mmol])**
	Urine sediment abnormalities
	Electrolyte and other abnormalities due to tubular disorders
	Abnormalities detected by histology
	Structural abnormalities detected by imaging
	History of kidney transplantation
Decreased glomerular filtration rate (GFR)	**GFR < 60 mL/min/1.73 m^2 (GFR categories G3a–G5)**

(Chapter1: Definition and classification CKD, *Kidney Int suppl*, 2013, p5)

Table II. Phenotypes seen in the appearance of WT and GMF-TG mice during the experimental period of 155 weeks.

	Alopecia	Skin atrophy	Spinal curvature
GMF-TG (n=97)	**n=17 (18%)**	**n=9 (9%)**	**n=9 (9%)**
WT (n=41)	**n=6 (15%)**	**n=0 (0%)**	**n=0 (0%)**

There were no detectable differences in body size, jaws or limbs between the WT and GMF-TG mice during the study.

References

1. Lim R, Mitsunobu K, Li WK: Maturation-stimulation effect of brain extract and dibutyryl cyclic AMP on dissociated embryonic brain cells in culture. Exp Cell Res 79: 243-246, (1973).
2. Lim R, Mitsunobu K: Brain cells in culture: morphological transformation by a protein. Science 185: 63-66, (1974).
3. Lim R, Nakagawa S, Arnason BG, et al.: Glia maturation factor promotes contact inhibition in cancer cells. Proc Natl Acad Sci U S A 78: 4373-4377, (1981).
4. Zaheer A, Zaheer S, Sahu SK, et al.: A novel role of glia maturation factor: induction of granulocyte-macrophage colony-stimulating factor and pro-inflammatory cytokines. J Neurochem 101: 364-376, (2007).
5. Lim R, Zaheer A, Yorek MA, et al.: Activation of nuclear factor-kappaB in C6 rat glioma cells after transfection with glia maturation factor. J Neurochem 74: 596-602, (2000).
6. Zaheer A, Fink BD, Lim R: Expression of glia maturation factor beta mRNA and protein in rat organs and cells. J Neurochem 60: 914-920, (1993).
7. Lim R, Zaheer A: Phorbol ester stimulates rapid intracellular phosphorylation of glia maturation factor. Biochem Biophys Res Commun 211: 928-934, (1995).
8. Zaheer A, Lim R: In vitro inhibition of MAP kinase (ERK1/ERK2) activity by phosphorylated glia maturation factor (GMF). Biochemistry 35: 6283-6288, (1996).
9. Lim R, Zaheer A: In vitro enhancement of p38 mitogen-activated protein kinase activity by phosphorylated glia maturation factor. J Biol Chem 271: 22953-22956, (1996).

10. Munshi A, Ramesh R: Mitogen-activated protein kinases and their role in radiation response. Genes Cancer 4: 401-408, (2013).
11. Zaheer A, Yorek MA, Lim R: Effects of glia maturation factor overexpression in primary astrocytes on MAP kinase activation, transcription factor activation, and neurotrophin secretion. Neurochem Res 26: 1293-1299, (2001).
12. Kempe S, Kestler H, Lasar A, et al.: NF-kappaB controls the global pro-inflammatory response in endothelial cells: evidence for the regulation of a pro-atherogenic program. Nucleic Acids Res 33: 5308-5319, (2005).
13. Poukkula M, Kremneva E, Serlachius M, et al.: Actin-depolymerizing factor homology domain: a conserved fold performing diverse roles in cytoskeletal dynamics. Cytoskeleton (Hoboken) 68: 471-490, (2011).
14. Kim J, Shapiro MJ, Bamidele AO, et al.: Coactosin-like 1 antagonizes cofilin to promote lamellipodial protrusion at the immune synapse. PLoS One 9: e85090, (2014).
15. Sirotkin V: Cell biology: actin keeps endocytosis on a short leash. Curr Biol 21: R552-554, (2011).
16. Takenaka M, Imai E, Kaneko T, et al.: Isolation of genes identified in mouse renal proximal tubule by comparing different gene expression profiles. Kidney Int 53: 562-572, (1998).
17. Nakajima H, Takenaka M, Kaimori JY, et al.: Gene expression profile of renal proximal tubules regulated by proteinuria. Kidney Int 61: 1577-1587, (2002).
18. Kaimori JY, Takenaka M, Nakajima H, et al.: Induction of glia maturation factor-beta in proximal tubular cells leads to vulnerability to oxidative injury through the p38 pathway and changes in antioxidant enzyme activities. J Biol Chem 278:

33519-33527, (2003).

19. Zaheer A, Yang B, Cao X, et al.: Decreased copper-zinc superoxide dismutase activity and increased resistance to oxidative stress in glia maturation factor-null astrocytes. Neurochem Res 29: 1473-1480, (2004).

20. De Marchi E, Baldassari F, Bononi A, et al.: Oxidative stress in cardiovascular diseases and obesity: role of p66Shc and protein kinase C. Oxid Med Cell Longev 2013: 564961, (2013).

21. Poljsak B, Suput D, Milisav I: Achieving the balance between ROS and antioxidants: when to use the synthetic antioxidants. Oxid Med Cell Longev 2013: 956792, (2013).

22. Le Bras M, Clement MV, Pervaiz S, et al.: Reactive oxygen species and the mitochondrial signaling pathway of cell death. Histol Histopathol 20: 205-219, (2005).

23. Chen JH, Hales CN, Ozanne SE: DNA damage, cellular senescence and organismal ageing: causal or correlative? Nucleic Acids Res 35: 7417-7428, (2007).

24. Pelicci PG: Do tumor-suppressive mechanisms contribute to organism aging by inducing stem cell senescence? J Clin Invest 113: 4-7, (2004).

25. Chapter 1: Definition and classification of CKD. Kidney Int Suppl (2011) 3: 19-62, (2013).

26. Ruggenenti P, Perna A, Mosconi L, et al.: Urinary protein excretion rate is the best independent predictor of ESRF in non-diabetic proteinuric chronic nephropathies. "Gruppo Italiano di Studi Epidemiologici in Nefrologia" (GISEN). Kidney Int 53: 1209-1216, (1998).

27. Dounousi E, Papavasiliou E, Makedou A, et al.: Oxidative stress is progressively

enhanced with advancing stages of CKD. Am J Kidney Dis 48: 752-760, (2006).

28. Kao MP, Ang DS, Pall A, et al.: Oxidative stress in renal dysfunction: mechanisms, clinical sequelae and therapeutic options. J Hum Hypertens 24: 1-8, (2010).

29. Zaheer S, Thangavel R, Sahu SK, et al.: Augmented expression of glia maturation factor in Alzheimer's disease. Neuroscience 194: 227-233, (2011).

30. Thangavel R, Kempuraj D, Stolmeier D, et al.: Glia maturation factor expression in entorhinal cortex of Alzheimer's disease brain. Neurochem Res 38: 1777-1784, (2013).

31. Stolmeier D, Thangavel R, Anantharam P, et al.: Glia maturation factor expression in hippocampus of human Alzheimer's disease. Neurochem Res 38: 1580-1589, (2013).

32. Zaheer A, Sahu SK, Wu Y, et al.: Diminished cytokine and chemokine expression in the central nervous system of GMF-deficient mice with experimental autoimmune encephalomyelitis. Brain Res 1144: 239-247, (2007).

33. Zaheer A, Zaheer S, Thangavel R, et al.: Glia maturation factor modulates beta-amyloid-induced glial activation, inflammatory cytokine/chemokine production and neuronal damage. Brain Res 1208: 192-203, (2008).

34. Kempuraj D, Khan MM, Thangavel R, et al.: Glia maturation factor induces interleukin-33 release from astrocytes: implications for neurodegenerative diseases. J Neuroimmune Pharmacol 8: 643-650, (2013).

35. Khan MM, Kempuraj D, Zaheer S, et al.: Glia maturation factor deficiency suppresses 1-methyl-4-phenylpyridinium-induced oxidative stress in astrocytes. J Mol Neurosci 53: 590-599, (2014).

36. Khan MM, Zaheer S, Nehman J, et al.: Suppression of glia maturation factor

expression prevents 1-methyl-4-phenylpyridinium (MPP(+))-induced loss of mesencephalic dopaminergic neurons. Neuroscience 277: 196-205, (2014).

37. Zaheer A, Mathur SN, Lim R: Overexpression of glia maturation factor in astrocytes leads to immune activation of microglia through secretion of granulocyte-macrophage-colony stimulating factor. Biochem Biophys Res Commun 294: 238-244, (2002).

38. Zaheer A, Zaheer S, Sahu SK, et al.: Reduced severity of experimental autoimmune encephalomyelitis in GMF-deficient mice. Neurochem Res 32: 39-47, (2007).

39. Verstraeten VL, Ji JY, Cummings KS, et al.: Increased mechanosensitivity and nuclear stiffness in Hutchinson-Gilford progeria cells: effects of farnesyltransferase inhibitors. Aging Cell 7: 383-393, (2008).

40. Sullivan T, Escalante-Alcalde D, Bhatt H, et al.: Loss of A-type lamin expression compromises nuclear envelope integrity leading to muscular dystrophy. J Cell Biol 147: 913-920, (1999).

41. Goldman RD, Gruenbaum Y, Moir RD, et al.: Nuclear lamins: building blocks of nuclear architecture. Genes Dev 16: 533-547, (2002).

42. Broers JL, Ramaekers FC, Bonne G, et al.: Nuclear lamins: laminopathies and their role in premature ageing. Physiol Rev 86: 967-1008, (2006).

43. Prokocimer M, Barkan R, Gruenbaum Y: Hutchinson-Gilford progeria syndrome through the lens of transcription. Aging Cell 12: 533-543, (2013).

44. Merideth MA, Gordon LB, Clauss S, et al.: Phenotype and course of Hutchinson-Gilford progeria syndrome. N Engl J Med 358: 592-604, (2008).

45. Navarro CL, Cadinanos J, De Sandre-Giovannoli A, et al.: Loss of ZMPSTE24 (FACE-1) causes autosomal recessive restrictive dermopathy and accumulation of

Lamin A precursors. Hum Mol Genet 14: 1503-1513, (2005).

46. Scaffidi P, Misteli T: Lamin A-dependent nuclear defects in human aging. Science 312: 1059-1063, (2006).

47. McClintock D, Ratner D, Lokuge M, et al.: The mutant form of lamin A that causes Hutchinson-Gilford progeria is a biomarker of cellular aging in human skin. PLoS One 2: e1269, (2007).

48. Ragnauth CD, Warren DT, Liu Y, et al.: Prelamin A acts to accelerate smooth muscle cell senescence and is a novel biomarker of human vascular aging. Circulation 121: 2200-2210, (2010).

49. Lattanzi G, Ortolani M, Columbaro M, et al.: Centenarian lamins: rapamycin targets in longevity. J Cell Sci, (2013).

50. Niwa H, Yamamura K, Miyazaki J: Efficient selection for high-expression transfectants with a novel eukaryotic vector. Gene 108: 193-199, (1991).

51. Franco NH, Correia-Neves M, Olsson IA: Animal welfare in studies on murine tuberculosis: assessing progress over a 12-year period and the need for further improvement. PLoS One 7: e47723, (2012).

52. Takeda T, Hosokawa M, Takeshita S, et al.: A new murine model of accelerated senescence. Mech Ageing Dev 17: 183-194, (1981).

53. Li AL, Li HY, Jin BF, et al.: A novel eIF5A complex functions as a regulator of p53 and p53-dependent apoptosis. J Biol Chem 279: 49251-49258, (2004).

54. Mounkes LC, Kozlov S, Hernandez L, et al.: A progeroid syndrome in mice is caused by defects in A-type lamins. Nature 423: 298-301, (2003).

55. Tyner SD, Venkatachalam S, Choi J, et al.: p53 mutant mice that display early ageing-associated phenotypes. Nature 415: 45-53, (2002).

56. Kondratov RV, Kondratova AA, Gorbacheva VY, et al.: Early aging and age-related pathologies in mice deficient in BMAL1, the core componentof the circadian clock. Genes Dev 20: 1868-1873, (2006).

57. Li L, Zhao D, Wei H, et al.: REGgamma deficiency promotes premature aging via the casein kinase 1 pathway. Proc Natl Acad Sci U S A 110: 11005-11010, (2013).

58. Lee YF, Liu S, Liu NC, et al.: Premature aging with impaired oxidative stress defense in mice lacking TR4. Am J Physiol Endocrinol Metab 301: E91-98, (2011).

59. Ruiz-Torres MP, Bosch RJ, O'Valle F, et al.: Age-related increase in expression of TGF-beta1 in the rat kidney: relationship to morphologic changes. J Am Soc Nephrol 9: 782-791, (1998).

60. Lim JH, Kim EN, Kim MY, et al.: Age-associated molecular changes in the kidney in aged mice. Oxid Med Cell Longev 2012: 171383, (2012).

61. Varela I, Cadinanos J, Pendas AM, et al.: Accelerated ageing in mice deficient in Zmpste24 protease is linked to p53 signalling activation. Nature 437: 564-568, (2005).

62. Zhang H, Kieckhaefer JE, Cao K: Mouse models of laminopathies. Aging Cell 12: 2-10, (2013).

63. Fong LG, Ng JK, Meta M, et al.: Heterozygosity for Lmna deficiency eliminates the progeria-like phenotypes in Zmpste24-deficient mice. Proc Natl Acad Sci U S A 101: 18111-18116, (2004).

64. Vijg J, Campisi J: Puzzles, promises and a cure for ageing. Nature 454: 1065-1071, (2008).

65. Sahin E, Depinho RA: Linking functional decline of telomeres, mitochondria and stem cells during ageing. Nature 464: 520-528, (2010).

66. Kudlow BA, Stanfel MN, Burtner CR, et al.: Suppression of proliferative defects associated with processing-defective lamin A mutants by hTERT or inactivation of p53. Mol Biol Cell 19: 5238-5248, (2008).

67. Sullivan KD, Gallant-Behm CL, Henry RE, et al.: The p53 circuit board. Biochim Biophys Acta 1825: 229-244, (2012).

68. Chan HM, Narita M, Lowe SW, et al.: The p400 E1A-associated protein is a novel component of the p53 --> p21 senescence pathway. Genes Dev 19: 196-201, (2005).

69. Mattera L, Courilleau C, Legube G, et al.: The E1A-associated p400 protein modulates cell fate decisions by the regulation of ROS homeostasis. PLoS Genet 6: e1000983, (2010).

70. Bergo MO, Gavino B, Ross J, et al.: Zmpste24 deficiency in mice causes spontaneous bone fractures, muscle weakness, and a prelamin A processing defect. Proc Natl Acad Sci U S A 99: 13049-13054, (2002).

List of publications

Rika Imai, Kanae Asai, Jun-ichi Hanai and Masaru Takenaka: Transgenic mice overexpressing glia maturation factor-β, an oxidative stress inducible gene, show premature aging due to Zmpste24 down-regulation. Aging (Albany NY) 7: 486-499, (2015).

Acknowledgements

First and foremost, I am deeply grateful to Dr. Masaru Takenaka, Professor of Kobe Women’s University, for his continuous guidance, invaluable discussion, limitless support, and critical reading of this thesis. At the same time, I would like to thank him for giving me this opportunity to have this great experience of studying in Kobe Women’s University.

I would also most grateful to Dr. Yasuhiko Okimura, Dr. Yuriko Kano and Dr. Haruko Nagasawa, Professors of Kobe Women’s University and Dr. Yasuhiro Inoue, Professor of Nara Women's University, for their valuable comments and advice.

I would also like to express my gratitude to Dr. Jun-ichi Hanai at Harvard Medical School & Beth Israel Deaconess Medical Center Renal Division & IMBIO, for his constructive opinion and suggestion throughout this work.

I am also indebted to Ms. Kanae Asai at Department of Metabolism and Clinical Nutrition, Kyoto University Hospital, for providing valuable experimental data.

I would also like to thank Ms. Yumiko Iwasaka, Assistant of Kobe Women’s University, for her helpful advice.

This work was financially supported by the Grants-in-aid for Scientific Research program sponsored by the Ministry of Education, Culture, Sports, Science and Technology of Japan, and the Technology of Japan and Nestlé Nutrition Council, Japan (NNCJ). The experiments in this study were performed at the Laboratory of Clinical Nutrition and Internal Medicine, Department of Nutrition and Food Science, Graduate School of Life Science, Kobe Women's University. I must also thank all those who gave

me the possibility to complete this thesis.

Finally, I would like to thank my parents and family for their unconditional support and encouragement.